Molecular Diversity
https://doi.org/10.1007/s11030-022-10548-9

ORIGINAL ARTICLE

Synthesis of new 3-acetyl-1,3,4-oxadiazolines combined with pyrimidines as antileishmanial and antiviral agents

Saida Lachhab[1] · Az-eddine El Mansouri[2] · Ahmad Mehdi[3] · Indira Dennemont[4] · Johan Neyts[5] · Dirk Jochmans[5] · Graciela Andrei[5] · Robert Snoeck[5] · Yogesh S. Sanghvi[6] · Mustapha Ait Ali[1] · Philippe M. Loiseau[4] · Hassan B. Lazrek[1]

Received: 12 June 2022 / Accepted: 7 October 2022

Abstract

A new series of 3-acetyl-1,3,4-oxadiazoline hybrid molecules was designed and synthesized using a condensation between acyclonucleosides and substituted phenylhydrazone. All intermediates and final products were screened against *Leishmania donovani*, a Protozoan parasite and against three viruses SARS-CoV-2, HCMV and VZV. While no significant activity was observed against the viruses, the intermediate with 6-azatymine as thymine and 5-azathymine-3-acetyl-1,3,4-oxadiazoline hybrid exhibited a significant antileishmanial activity. The later compound was the most promising, exhibiting an IC_{50} value at 8.98 µM on *L. donovani* intramacrophage amastigotes and a moderate selectivity index value at 2.4.

Graphical Abstract

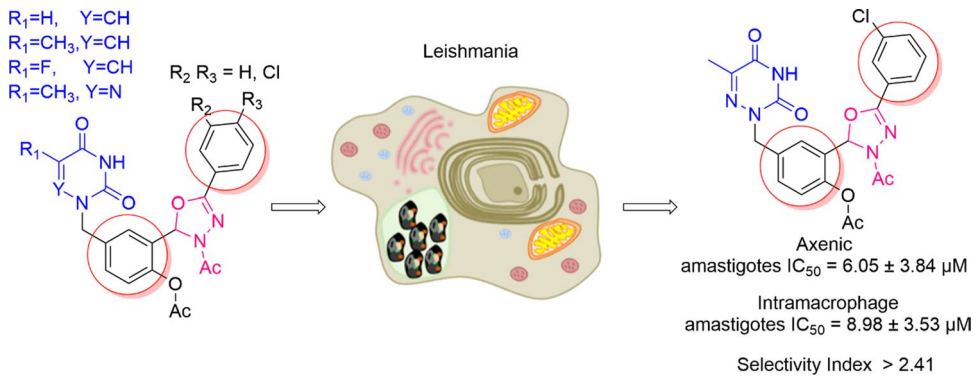

Keywords 3-Acetyl-1,3,4-oxadiazoline · Pyrimidines analogs · Antileishmanial activity · Antiviral activity

✉ Hassan B. Lazrek
hblazrek50@gmail.com

[1] Laboratory of Biomolecular and Medicinal Chemistry, Faculty of Science Semlalia, University Cadi Ayyad, Marrakech, Morocco

[2] Department of Chemistry, University of the Free State, P.O. Box 339, Bloemfontein 9300, South Africa

[3] ICGM, Université Montpellier, CNRS, ENSCM, Montpellier, France

[4] Antiparasite Chemotherapy, CNRS, BioCIS, Université Paris-Saclay, Chatenay-Malabry, 92290 Paris, France

[5] Rega Institute for Medical Research, KULeuven, Louvain, Belgium

[6] Rasayan Inc., 2802 Crystal Ridge Road, Encinitas, CA 92024-6615, USA

Published online: 17 October 2022

Introduction

Neglected tropical diseases (NTDs) are widespread in several countries in Africa, Europe, America, and Asia. Every year, NTDs contaminate millions of people in 149 countries, which cause wasting billions of dollars and claiming thousands of lives [1]. According to the World Health Organization (WHO), leishmaniases are a class of illnesses prompted by the Protozoan parasite Leishmania, showing four crucial clinical syndromes: post kala azar dermal leishmaniasis (PKDL), cutaneous leishmaniasis (CL), visceral leishmaniasis/kala azar (VL), and mucocutaneous leishmaniasis (MCL) [2].

On the other hand, the immune system response to the illnesses is altered by co-infection with the human immunodeficiency virus, HIV [3]. Furthermore, leishmaniases have an increased medical value in infected people with HIV-1 (human immunodeficiency virus type 1) because of the spread of both pathogens in several regions of the world (e.g., South America, India, the Mediterranean Basin, and many African countries). There is absolutely no doubt that the exact number of reported cases of co-infection is undercounted due to various issues with HIV-1 infection, leishmaniasis, or both in the setting of developing countries [4]. Ellen Heirwegh et al., reported that *Leishmania major* with phleboviral infection was more infectious than *L. major* alone. A better understanding of the possible role of viral co-infection might lead to more effective treatment regimens [5]. One of the key challenges in the management of leishmaniasis and viral disease co-infection is the invention of a clinically effective treatment that not only treats leishmaniasis but also prevents viral disease. However, there is a lack of knowledge on the correlation between leishmaniasis and viral disease co-infection. Moreover, Antonis Pikoulas et al., presented a case of co-infection with COVID-19 and visceral leishmaniasis, and discuss recent reports on co-existence of leishmania and SARS-CoV2 spp. to date [6].

Current treatments for visceral leishmaniasis including antimonials, liposomal amphotericin B, miltefosine, and paromomycin, have some issues related to toxicity, emerging resistance, high cost and relatively long treatment regimens. Therefore, there is an urgent need for the development of new and better medicines [7, 8].

1,3,4-Oxadiazoles are a very important series in chemistry as they have several biological activities. The 1,3,4-oxadiazole scaffold is present in numerous drugs: Nesapidil® (anti-hypertensive) [9], Furamizol® (antibiotic) [10], Raltegravir® (anti-retroviral) [11], and Zibotentan® (anticancer) [12, 13]. We also notice that the *N*-acetyl-1,3,4-oxadiazoline is among the derivatives of 1,3,4-oxadiazoles that showed different antileishmanial activities. For instance, Taha et al. have synthesized phenyl-linked oxadiazoline–phenylhydrazone hybrids **I** as the most potential antileishmanial candidate, with an IC_{50} value of 0.95 ± 0.01 µM [14]. Moreover, another series of quinolinyl–oxadiazole hybrids had promising antileishmanial activities, and compound **II** emerged as the most potent agent with an IC_{50} value of 0.10 ± 0.001 µM [15]. Meanwhile, some *N*-acetyl-1,3,4-oxadiazoline derivatives have been reported as antiviral agents. For instance, Ali et al. prepared a series of monosaccharide 1-acetylhydrazinouracils that was evaluated for antiviral activity against hepatitis B virus and showed moderate activities **III** [16]. Moreover, they showed activities as antibacterial [17, 18], antimicrobial [19, 20], antifungal [21], and anti-inflammatory [22] (Fig. 1).

Substituted pyrimidines are widely available in living organisms and are one of the most important compounds studied by chemists. Pyrimidines, including thymine, uracil, and derivatives, are among the most abundant heterocyclic diazines. According to the literature, pyrimidine derivatives exhibit a wide range of pharmacological properties, including antifungal activity [23, 24], antibacterial [25, 26], antileishmanial [27], antiviral [28, 29], and anticancer [30, 31]. A rational discovery of novel antiparasitic drugs should be based on parasite-specific metabolisms [32]. The biosynthesis of pyrimidine is a biologically important process that occurs via both de novo production and pyrimidine salvage routes. The enzymes of this pathway are considered potential drug targets. Meanwhile, several studies have shown that pyrimidines have widely antileishmanial activities. For instance, the synthesis of pyrimidine derivatives led to the discovery of the potent compound **P1** (Fig. 2) with an EC_{50} value of 0.65 µM against intracellular *Leishmania donovani* amastigotes [33]. Moreover, pyrimidines **P2** have been demonstrated to be efficacious in vivo, with each compound leading to 78% parasite inhibition when dosed in *L. donovani* infected hamsters for five days (50 mg kg^{-1}, i.p.) [34]. Finally, Chauhan and coworkers have described that aza-pyrimidine–pentamidine hybrids **P3** have promising activity on intracellular *L. donovani* amastigotes (EC_{50} values of < 1 µM) [35].

Prompted with these literature reports, we designed some novel hybrid molecules which combined the pyrimidine and 3-acetyl-1,3,4-oxadiazoline scaffolds in order to investigate firstly their in vitro antileishmanial activity against the axenic amastigotes and intramacrophage amastigotes forms of *L. donovani*, and second, their antiviral activity against SARS-CoV-2, HCMV, and VZV (Fig. 3).

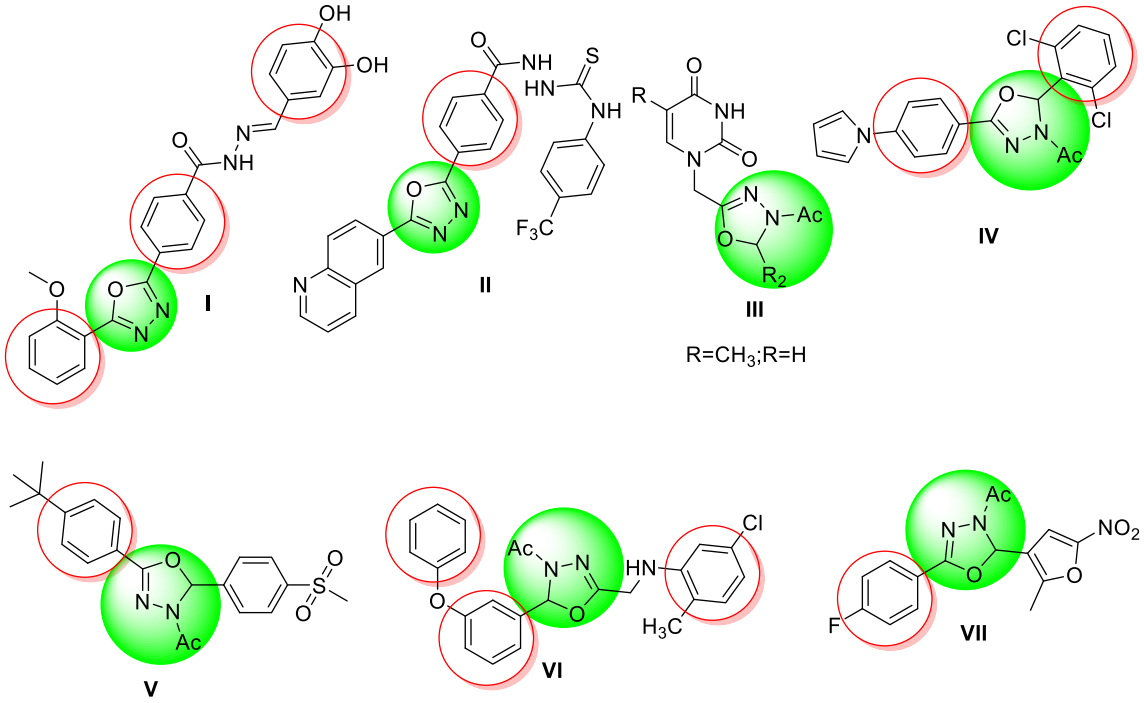

Fig. 1 Structures of some bioactive 1,3,4-oxadiazoline based hybrids

Fig. 2 Structures of some bioactive pyrimidine-based hybrids

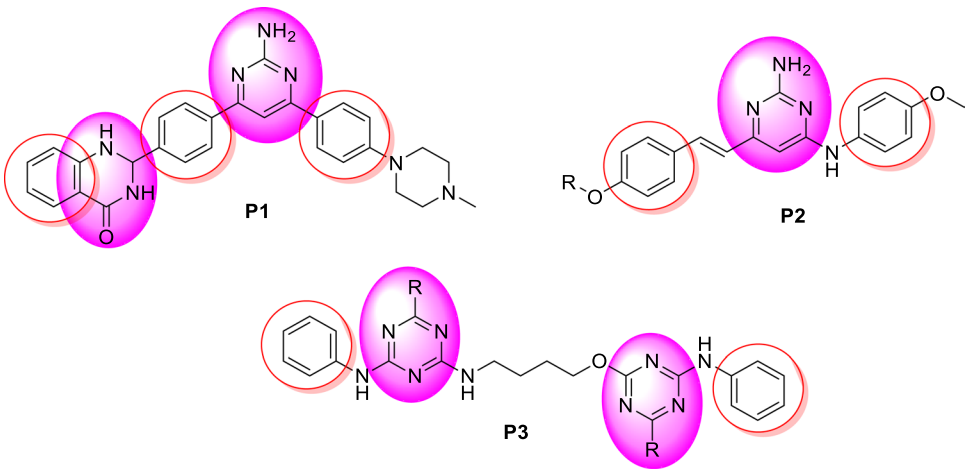

Results and discussion

Chemistry

The synthetic strategy to achieve compounds (**14–23**) is shown in Schemes 1, 2, and 3. The crucial step for synthesizing acyclonucleosides derivatives (**7–10**) (Scheme 1) known as modified Hilbert-Johnson reaction [36] corresponded to the condensation between silylated nucleobases (**3′–6′**) and alkylating agent **2** [37]. The desired products were obtained in synthetically good yields between 53 and 84%. Thereafter, the methyl benzoate derivatives (**11″–13″**) were subjected to a hydrazinolysis reaction after treatment with 80% aqueous hydrazine hydrate in ethanol under reflux to afford the corresponding hydrazides (**11–13**) in good yield (Scheme 2). The latter were reacted with the aldehyde derivatives (**7–10**) to give the imine derivatives (**14′–23′**) which were treated with acetic anhydride under heating (155 °C) to promote cyclization and furnished the *N*3-acetyl-1,3,4-oxadiazoline derivatives (**14–23**) in yield ranging from 40 to 71%. All the oxadiazoles were completely characterized using NMR (^{13}C and ^{1}H), IR, and high-resolution mass spectrometry.

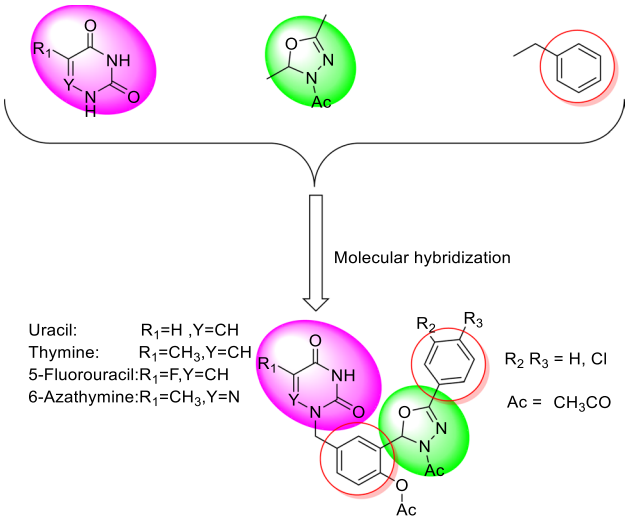

Fig. 3 Design of new *N*-acetyl 1,3,4-oxadiazoline–pyrimidine hybrids

In the ^{1}H NMR spectra, the signal for the hydrogen present in the oxadiazole ring (H-2) was observed within the 7.20–7.67 ppm range. The hydrogen atoms of methylene group attached to nitrogen (nucleobases) were noticed as singlet in the ^{1}H NMR spectra. The carbon chemical shifts are compatible with the structures of the compounds. In the IR spectra, expected bands for functional groups were noticed. The exact mass of the hybrid molecules (**14–23**) was confirmed by high-resolution mass spectrometry analyses.

Biological evaluation

Antileishmanial activity

The novel series of nucleosides analogs of 3-acetyl-1,3,4-oxadiazoline **14–23** and alkylated pyrimidines (uracil, thymine, 5-fluorouracil, and 5-azathymine) **7–10** were tested for their biological activity. This series was not highly cytotoxic on the RAW 264.7 macrophage model since eleven compounds exhibited CC_{50} values superior to 100 µM. However, the most cytotoxic (compounds **10, 20, 23**) with CC_{50} values in a range from 19 to 56 µM, were the single ones having a significant antileishmanial activity against the axenic amastigotes and intramacrophage amastigotes forms of *L. donovani.*

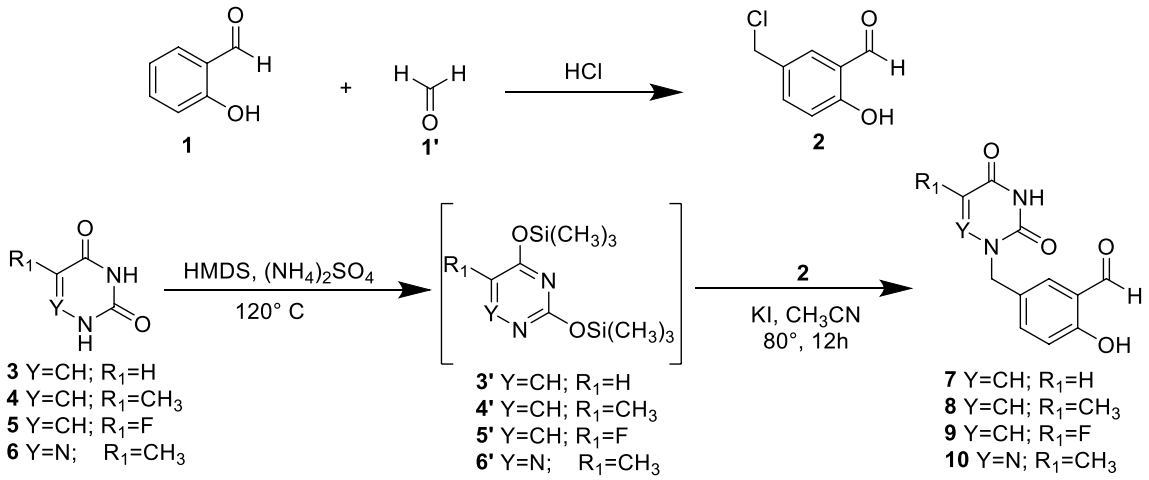

Scheme 1 Synthesis of compound **2** and N1-alkylated pyrimidines **7–10**

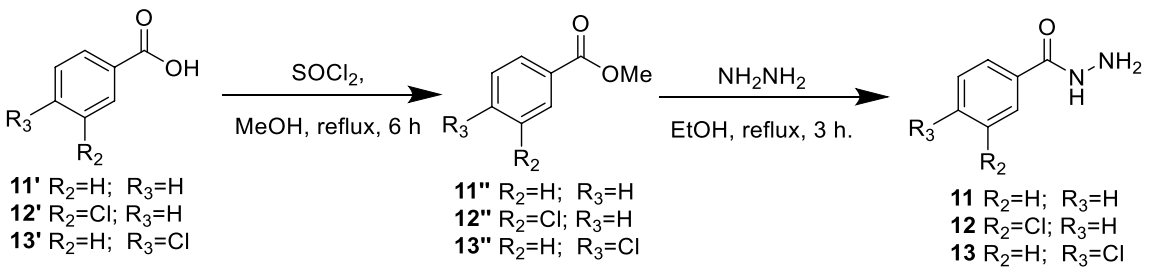

Scheme 2 Synthesis of hydrazide derivatives **11–13**

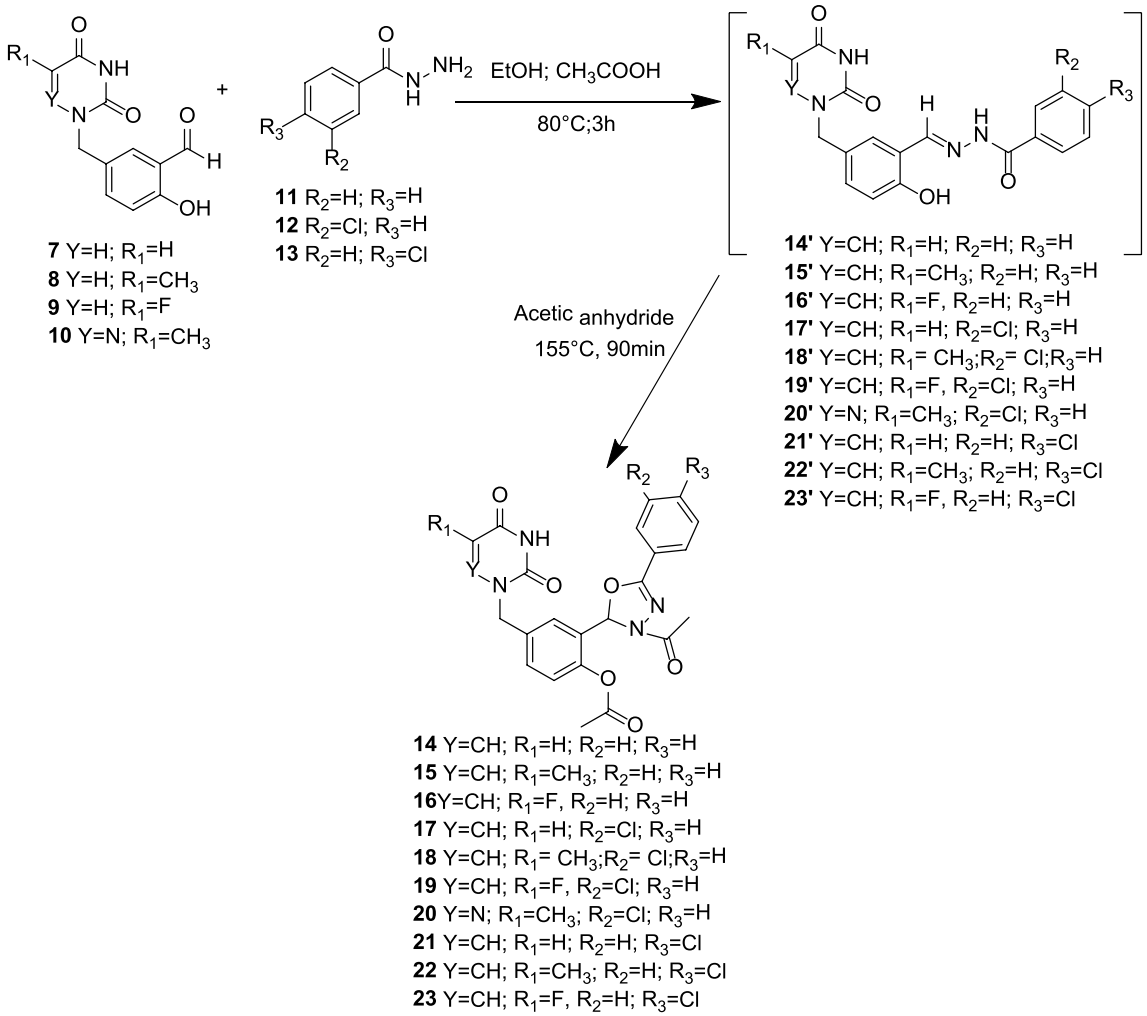

Scheme 3 Preparation of 3-acetyl-1,3,4-oxadiazoline–pyrimidine hybrids **14–23**

The IC_{50} and CC_{50} values of the compounds were compared to those of miltefosine as the reference drug. The results, presented in Table 1, clearly showed that the starting material compound **10** presented a moderate activity (CC_{50} = 56.15 µM, IC_{50} = 29.02 µM (Axenic amastigotes), IC_{50} = 29.96 µM (intramacrophage amastigotes), and SI = 1.87). It is worth to note that when thymine as a nucleobase **8** was changed to 6-azathymine **10,** the IC_{50} decrease from 100 to 29.02 µM. Furthermore, when the oxadiazole group is introduced in the hybrid molecule **20,** the IC_{50} decrease from 29.02 to 6.05 µM. The most active derivatives **20** showed a significant activity: IC_{50} = 6.05 µM (Axenic amastigotes) and IC_{50} = 8.98 µM (Intramacrophage amastigotes) CC_{50} = 21.66 µM and very moderate selectivity index value of up to 2.41 comparatively to miltefosine (Table 1).

The structure–activity relationship showed that oxadiazole derivatives **14–23** had better activity than the acyclonucleosides **7–10**. As a result, it was concluded that the creation of a stereoisomer center C_2 on the oxadiazole ring may influence the antileishmanial activity, this was supported by the fact that the oxadiazole derivative **20** was 5 times more potent than the acyclonucleoside derivative **10**. From the biological data collected with derivatives **19** and **23** having 5-fluorouracil as a nucleobase, SARs showed that, at the *para* position of the phenyl moiety, the chlorine substituent was favorable while the *meta*-chlorine was not suitable for providing antileishmanial activity.

Moreover, a comparison of the activity profiles of compounds **10** and **20** draws speculation that the oxadiazole group may be serving as a chromophore group. Thus, additional modifications will be pursued in subsequent studies, as this approach has been shown to greatly enhance antileishmanial activity of oxadiazole analogs.

Determination of compound lipophilicity

There are physical differences between the test systems on promastigote and amastigote forms of *L. donovani*, which

Table 1 Cytotoxicity, antileishmanial activities of compounds **7–10** and **14–23** on axenic and intramacrophage forms of *Leishmania donovani* and selectivity index

Product	Cytotoxicity CC_{50}	Axenic amastigotes IC_{50}	Intramacrophage amastigotes IC_{50}	SI (CC_{50}/IC_{50})	*Clog*P
7	> 100	> 100	> 100	–	0.239
8	> 100	> 100	> 100	–	0.734
9	> 100	> 100	> 100	–	0.719
10	**56.15 ± 16.75**	**29.02 ± 2.84**	**29.96 ± 2.18**	**1.87**	**1.791**
14	> 100	> 100	> 100	–	1.015
15	> 100	> 100	> 100	–	1.514
16	> 100	> 100	> 100	–	1.494
17	> 100	> 100	> 100	–	1.728
18	> 100	> 100	> 100	–	2.227
19	> 100	> 100	> 100	–	2.207
20	**21.66 ± 3.11**	**6.05 ± 3.84**	**8.98 ± 3.53**	**2.41**	**3.28**
21	> 100	> 100	> 100	–	1.728
22	> 100	> 100	> 100	–	2.227
23	**19.16 ± 1.39**	**56.29 ± 3.20**	**> 19.16**	**< 1**	**2.207**
Miltefosine	**52.24 ± 11.08**	**0.51 ± 0.29**	**11.82 ± 2.43**	**> 4.41**	–

could explain the obtained results. The promastigote test employs an extracellular axenic parasite, which is more accessible than the intracellular amastigotes. Indeed, the parasite starts the creation of a membrane (parasitophorous vacuole membrane, which surrounds the intracellular parasite) during the invasion process. Permeation of the two membranes (plasmatic and vacuole) is a critical criterion for activity and varies depending on the hydrophobicity of the compound [38, 39].

The octanol/water partition coefficients (*Clog*P) reflect the hydrophobicity, and products that have higher *Clog*P are more lipophilic. Chemdraw was used to predict partition coefficients in this study. As shown in Table 1, we notice that the incorporation of 1,3,4-oxadiazoline increases the hydrophobic character. For instance, when we compare compound **10** and **20**, *Clog*P is enhanced by about two times, which explain that oxadiazoline **20** is more active than **10**. Similarly, by comparing all nucleobases, 6-azathymine is the most hydrophobic, which follows the results of biological activities.

Antiviral activity

All the synthesized compounds (**7–10**, **14–23**) were evaluated for their antiviral activities against human cytomegalovirus (HCMV) and human varicella-zoster virus (VZV), both thymidine kinase-deficient TK and wild type. The pyrimidine–1,3,4-oxadiazole hybrids were unable to substantially inhibit the replication of these two DNA viruses at non-toxic concentrations, in contrast to the compounds used as reference (Ganciclovir, and Cidofovir against for HCMV, and Acyclovir for VZV) (Tables 2, 3).

Only three compounds **10**, **17,** and **19** showed moderate activity against VZV with $EC_{50} = 46.95$ µM, 43.02 µM, and 34.38 µM, respectively. We notice that when the fluorine atom is present in the acyclonucleoside, the value of EC_{50} decreases from 43.02 µM for uracil acyclonucleoside **17** to 34.38 µM for 5-fluorouracil acyclonucleoside **19** (Table 2). Whereas only compound **10** is moderately active against HCMV with $EC_{50} = 63.14$ µM (AD-169 strain) and 44.72 µM (Davis strain) (Table 3).

The rapidly developing pandemic, known as coronavirus disease 2019 (COVID-19), is caused by the severe acute respiratory syndrome coronavirus 2 (SARS-CoV-2). The rapid global emergence of SARS-CoV-2 has advanced research efforts toward the development of therapeutic intervention and finding viral drug to control the pandemic. The functional importance of RNA-dependent RNA polymerase (RdRp) in the viral life cycle, makes it an attractive target for designing antiviral drugs. Moreover, SARS-CoV-2 is an RNA virus like HCV, HIV, and other flaviviruses that share a similar replication mechanism requiring an RNA-dependent RNA polymerase (RdRp). In addition, the most promising broad-spectrum class of viral RdRp inhibitors are nucleos(t)ide analogs [40, 41]. Elfiky used a molecular docking study to predict that Ribavirin, Remdesivir, Sofosbuvir, Galidesivir, and Tenofovir may have inhibitory activity against SARS-CoV-2 RdRp [42]. Significant efforts have been made to discover novel or repurposed therapeutics to select the best candidates for the management of COVID-19 disease. To date, the US Food and Drug Administration (US FDA) has proved eleven agents emergency for the treatment of COVID patients, including two nucleosides analogs: remdesivir and Beta-D-N4-hydroxycytidine (NHC, molnupiravir) [43]. In this context, all synthesized hybrid molecule analogs

Table 2 Anti-VZV activities of compounds **7–10** and **14–23**

Product	Antiviral activity EC_{50} (μM)[a]		Cytotoxicity (μM)	
	TK^+ VZV strain	TK^- VZV strain	Cell morphology	Cell growth
	OKA	07-1	(MCC)[b]	(CC_{50})[c]
7	> 100	> 100	> 100	ND
8	> 100	> 100	> 100	ND
9	> 100	> 100	> 100	ND
10	**46.95**	> 20	≥ 20	ND
14	> 100	> 100	≥ 100	ND
15	> 100	> 100	≥ 20	ND
16	> 100	> 100	> 100	ND
17	**43.02**	> 20	100	ND
18	> 20	> 20	100	ND
19	**34.38**	> 20	≥ 100	ND
20	> 20	> 20	100	ND
21	> 20	> 20	100	ND
22	> 20	> 20	100	ND
23	> 20	> 20	100	ND
Acyclovir (ACV)	6.26	46.80	> 444	> 444

[a]Effective concentration required to reduce virus plaque formation by 50%. Virus input was 20 plaque forming units (PFU)

[b]Minimum cytotoxic concentration that causes a microscopically detectable alteration of cell morphology

[c]Cytostatic concentration required to reduce cell growth by 50%

Table 3 Anti-HCMV activities of compounds **7–10** and **14–23**

Product	Antiviral activity EC_{50} (μM)[a]		Cytotoxicity (μM)	
	AD-169 strain	Davis strain	Cell morphology (MCC)[b]	Cell growth (CC_{50})[c]
7	> 100	> 100	≥ 100	ND
8	> 20	> 100	≥ 100	ND
9	> 100	> 100	100	ND
10	**63.14**	**44.72**	≥ 100	ND
14	> 100	> 100	100	ND
15	> 100	> 100	≥ 100	ND
16	> 100	> 100	100	ND
17	> 100	> 100	100	ND
18	> 20	> 20	100	ND
19	> 20	> 20	100	ND
20	> 20	> 20	≥ 20	ND
21	> 20	> 20	100	ND
22	> 20	> 20	≥ 20	ND
23	> 20	> 20	100	ND
Ganciclovir (GCV)	6.5 ± 1.77	1.64 ± 0.22	> 394	> 394
Cidofovir (CDV)	0.84 ± 0.21	0.12 ± 0.03	317	> 317

[a]Effective concentration required to reduce virus-induced cytopathic effect by 50%. Virus input was 100 plaque forming units (PFU)

[b]Minimum cytotoxic concentration that causes a microscopically detectable alteration of cell morphology

[c]Cytostatic concentration required to reduce cell growth by 50%

(**7–10**, **14–23**) were evaluated for their anti-SARS-CoV-2 activity against Beta-Cov/Belgium/GHB-03021/2020. All tested compounds showed no anti-SARS-CoV-2 activity, with $EC_{50} > 100$ µM.

Experimental section

Chemistry

General

Melting points have been measured without correction using a Büchi B-545 electronic capillary melting temperature apparatus. TLC was employed to check reactions utilizing aluminum sheets coated with Merck's silica gel 60 F254. FTIR spectra were taken on a Perkin-Elmer VERTEX 70 FTIR spectroscopy covering the frequency 400–4000 cm^{-1}. The spectrums of ^{1} H and ^{13}C NMR were recorded in DMSO-d_6 or $CDCl_3$ solution on a Bruker Advance 300 spectrometer at 300 and 75 MHz, respectively. Using DMSO-d_6 as an internal reference, the chemical shifts are displayed in parts per million (ppm). The next abbreviations represent the signal multiplicities: s = singlet, d = doublet, m = multiplet, t = triplet, q = quadruplet, and as well as the coupling constants *J*, are documented in Hertz. The used chemicals in the synthesis were purchased from Fluka and Sigma Aldrich.

HPLC/MS conditions HPLC/MS was performed on a Thermo Scientific Dionex Ultimate 3000 consisted of a quaternary (HPG-3400RS) pump, a WPS-3000 (TSL) analytical auto-sampler, a TCC-3000 column oven, and a TSQ Endura (Thermo Fisher Scientific) triple quadrupole equipped with heated-electrospray ionization (H-ESI). The separation was performed on a Eurospher II 100-5 C_{18} vertex plus column (250 4.6 mm, 5m) at 25 °C. The mobile phases were composed of acetonitrile (A) and water/0.1% formic acid (B) with an elution program as follows: 20% of (A) for 8.6 min and 85% of (A) for 5.4 min. The solvent system flow rate was set to 1.0 mL min^{-1}, and the sample injection volume was 20 L. UV–Vis detection was monitored at 260 nm, while DAD acquisition was done between 200 and 600 nm.

General procedure for the preparation of the 2-hydroxybenzaldehyde homonucleosides

The mixture of the pyrimidine base (1 mmol) (**3–6**) and ammonium sulfate (0.10 mmol, 10 mg) in hexamethyldisilazane (1 mL) was refluxed (3 h) at 120 °C to give a clear solution (silylation step). Then the benzyl derivative (2.5 mmol, 425 mg), KI (0.50 mmol, 84 mg) and the solvent (acetonitrile) (5 mL) were added. The mixture was heated at 85 °C for 12 h, diluted with dichloromethane/methanol, and evaporated to dryness. The residue was purified by flash chromatography (solvent CH_2Cl_2/MeOH 99/1).

5-((2,4-Dioxo-3,4-dihydropyrimidin-1(2*H*)-yl) methyl)-2-hydroxybenzaldehyde (7) $R_f = 0.26$ [CH_2Cl_2/MeOH (97/3)]. Yield = 84%, *m* = 207 mg. Mp = (218–220) °C. UV (methanol) $\lambda_{max} = 259$ nm. IR υ (cm^{-1}): 3020 (=CH); 1689 (C=O aldehyde); 1350 (CH_2). ^{1}H NMR (300 MHz, DMSO d-6) δ (ppm): 4.80 (s, 2H, CH_2); 5.57 (d, $^{3}J_{H-H} = 7.8$ Hz, 1H, H-5); 6.97 (d, $^{3}J_{H-H} = 8.4$ Hz, 1H, H_{Ph}); 7.47 (d, $^{3}J_{H-H} = 8.4$ Hz, 1H, H_{Ph}); 7.60 (s, 1H, H_{Ph}); 7.76 (d, $^{3}J_{H-H} = 7.8$ Hz, 1H, H-6); 10.25 (s, 1H, H-aldehyde); 10.77 (s, 1H, OH); 11.30 (s, 1H, H-3). ^{13}C NMR (75 MHz, DMSO-d_6) δ (ppm): 49.63 (CH_2); 101.22 (C-5); 117.63 (C_{Ph}); 122.20 (C_{Ph}); 127.84 (C_{Ph}); 127.93 (C_{Ph}); 135.94 (C_{Ph}); 145.40 (C-6); 150.95 (C-2); 160.40 (C_{Ph}); 163.59 (C-4); 190.80 (C-aldehyde). HPLC/MS (*m*/*z*) 247.07 $(M+H)^+$, HRMS for $C_{12}H_{11}N_2O_4$: Calc 247.0713, Found 247.0716.

2-Hydroxy-5-((5-methyl-2,4-dioxo-3,4-dihydropyrimidin-1(2*H*)-yl) methyl) benzaldehyde (8) $R_f = 0.38$ [CH_2Cl_2/MeOH (97/3)]. Yield = 76%, *m* = 198 mg. Mp = (218–220) °C. UV (methanol) $\lambda_{max} = 259$ nm. IR υ (cm^{-1}): 3053 (=CH); 1696 (C=O aldehyde); 1364 (CH_2). ^{1}H NMR (300 MHz, DMSO d-6) δ (ppm): 1.74 (s, 3H, CH_3); 4.76 (s, 2H, CH_2); 6.97 (d, $^{3}J_{H-H} = 8.4$ Hz, 1H, H_{Ph}); 7.47 (d, $^{3}J_{H-H} = 8.4$ Hz, 1H, H_{Ph}); 7.59 (s, 1H, H-6); 7.63 (s, 1H, H_{Ph}); 10.24 (s, 1H, H-aldehyde); 10.76 (s, 1H, OH); 11.29 (s, 1H, H-3). ^{13}C NMR (75 MHz, DMSO d-6) δ (ppm): 11.88 (CH_3); 48.90 (CH_2); 109.00 (C-5); 117.62 (C_{Ph}); 122.09 (C_{Ph}); 127.95 (C_{Ph}); 128.02 (C_{Ph}); 135.92 (C_{Ph}); 141.07 (C-6); 150.95 (C-2); 160.30 (C_{Ph}); 164.17 (C-4); 190.99 (C-aldehyde). HPLC/MS (*m*/*z*) 261.08 $(M+H)^+$, HRMS for $C_{13}H_{13}N_2O_4$: Calc 261.0870, Found 261.0877.

5-((5-Fluoro-2,4-dioxo-3,4-dihydropyrimidin-1(2*H*)-yl) methyl)-2-hydroxybenzaldehyde (9) $R_f = 0.37$ [CH_2Cl_2/MeOH (97/3)]. Yield = 72%, *m* = 190 mg. Mp = (236–238) °C. UV (methanol) $\lambda_{max} = 258$ nm. IR υ (cm^{-1}): 3026 (=CH); 1691 (C=O aldehyde); 1348 (CH_2). ^{1}H NMR (300 MHz, DMSO d-6) δ (ppm): 4.75 (s, 2H, CH_2); 6.97 (d, $^{3}J_{H-H} = 8.4$ Hz, 1H, H_{Ph}); 7.49 (d, $^{3}J_{H-H} = 8.4$ Hz, 1H, H_{Ph}); 7.63 (s, 1H, H_{Ph}); 8.21 (d, $^{3}J_{H-F} = 6.9$ Hz, 1H, H-6); 10.24 (s, 1H, H-aldehyde); 10.78 (s, 1H, OH); 11.82 (s, 1H, H-3). ^{13}C NMR (75 MHz, DMSO d-6) δ (ppm): 48.61 (CH_2); 117.59 (C_{Ph}); 122.10 (C_{Ph}); 127.37 (C_{Ph}); 128.27 (C_{Ph}); 129.60 (d, $^{2}J_{C-F} = 32.7$ Hz, C-6); 136.03 (C_{Ph}); 138.21 (d, $^{1}J_{C-F} = 230.85$, C-5); 149.58 (C-2); 160.30 (C_{Ph}); 157.16 (d, $^{2}J_{C-F} = 25.75$ Hz, C-4); 190.82 (C-aldehyde). HPLC/MS (*m*/*z*) 265.06 $(M+H)^+$, HRMS for $C_{12}H_{10}FN_2O_4$: Calc 265.0619, Found 265.0623.

2-Hydroxy-5-((6-methyl-3,5-dioxo-4,5-dihydro-1,2,4-triazin-2(3*H*)-yl) methyl) benzaldehyde (10) $R_f = 0.47$ [CH_2Cl_2/MeOH (97/3)]. Yield = 53%, $m = 138$ mg. Mp = (198–200) °C. UV (methanol) $\lambda_{max} = 258$ nm. IR υ (cm^{-1}): 3018(=CH); 1664 (C=O aldehyde); 1379 (CH_2). ^{1}H NMR (300 MHz, DMSO d-6) δ (ppm): 2.05 (s, 3H, CH_3); 4.92 (s, 2H, CH_2); 6.95 (d, $^3J_{H-H} = 8.7$ Hz, 1H, H_{Ph}); 7.45 (d, $^3J_{H-H} = 8.4$ Hz, 1H, H_{Ph}); 7.59 (s, 1H, H_{Ph}); 10.23 (s, 1H, H-aldehyde); 10.75 (s, 1H, OH); 12.11 (s, 1H, H-3). ^{13}C NMR (75 MHz, DMSO d-6) δ (ppm): 15.85 (CH_3); 51.84 (CH_2); 117.46 (C_{Ph}); 122.00 (C_{Ph}); 127.77 (C_{Ph}); 128.27 (C_{Ph}); 135.94 (C_{Ph}); 143.44 (C-5); 148.69 (C-2); 157.02 (C-4); 160.21 (C_{ph}); 191.12 (C-aldehyde). HPLC/MS (*m*/*z*) 262.08 $(M+H)^+$, HRMS for $C_{12}H_{12}N_3O_4$: Calc 262.0822, Found 262.0823.

General procedure for the preparation of the *N*-acetyl 1,3,4 oxadiazol homonucleosides

A mixture of 2-hydroxy benzaldehyde homonucleosides (0.3 mmol) (**7–10**) and benzoic hydrazide acid (0.36 mmol) (**11–13**) was refluxed in ethanol (4 mL) for 3 h in the presence of catalytic amount of acetic acid (3 drops). The reaction mixture was evaporated to dryness, 3 mL of acetic anhydride added, and agitated at 155 °C for 90 min. The solution was poured into ice and neutralized with $NaHCO_3$. The obtained solid was filtered and purified by flash chromatography (CH_2Cl_2/MeOH 98/2).

2-(3-Acetyl-5-phenyl-2,3-dihydro-1,3,4-oxadiazol-2-yl)-4-((2,4-dioxo-3,4-dihydropyrimidin-1(2*H*)-yl) methyl) phenyl acetate (14) $R_f = 0.26$ [CH_2Cl_2/MeOH (97/3)]. Yield = 50%, $m = 67$ mg. Mp = (214–216) °C. UV (methanol) $\lambda_{max} = 271$ nm. IR υ (cm^{-1}): 3459 (NH); 1765 (C=O); 1690 (C=C); 691 (OH phenol). ^{1}H NMR (300 MHz, DMSO d-6) δ (ppm): 2.11 (s, 3H, CH_3); 2.19 (s, 3H, CH_3); 4.90 (s, 2H, CH_2); 5.62 (d, $^3J_{H-H} = 7.8$ Hz, 1H, H-5); 7.17 (s, 1H, H-oxadiazoline); 7.38 (d, 1H, $^3J_{H-H} = 7.8$ Hz, H-6); 7.49–7.80 (m, 8H, H-aromatic); 11.36 (s, 1H, H-3). ^{13}C NMR (75 MHz, DMSO d-6) δ (ppm): 20.44 (CH_3); 20.96 (CH_3); 49.56 (CH_2); 90.07 (C-oxadiazoline); 101.37 (C-5); 123.81 (C_{ph}); 124.35 (C_{ph}); 126.42 (C_{ph}); 128.19 (C_{ph}); 128.65 (C_{ph}); 129.10 (C_{ph}); 129.93 (C_{ph}); 131.90 (C_{ph}); 134.72 (C_{ph}); 145.44 (C-6); 148.22 (C_{ph}); 151.03 (C-2); 154.58 (C-oxadiazoline); 163.56 (C-4); 166.19 (CO acetyl); 168.55 (CO acetyl). HPLC/MS (*m*/*z*) 449.15 $(M+H)^+$, HRMS for $C_{23}H_{21}N_4O_6$: Calc 449.1456, Found 449.1453.

2-(3-Acetyl-5-phenyl-2,3-dihydro-1,3,4-oxadiazol-2-yl)-4-((5-methyl-2,4-dioxo-3,4-dihydropyrimidin-1(2*H*)-yl) methyl) phenyl acetate (15) $R_f = 0.31$ [CH_2Cl_2/MeOH (97/3)]. Yield = 71%, $m = 98$ mg. Mp = (231–233) °C. UV (methanol) $\lambda_{max} = 277$ nm. IR υ (cm^{-1}): 3463 (NH); 1767 (C=O); 1662 (C=C); 1196 (C–N); 693 (OH phenol). ^{1}H NMR (300 MHz, DMSO d-6) δ (ppm): 1.75 (CH_3); 2.11 (s, 3H, CH_3); 2.19 (s, 3H, CH_3); 4.87 (s, 2H, CH_2); 7.18 (s, 1H, H-oxadiazoline); 7.48 (s, 1H, H-6); 7.38–7.80 (m, 6H, H-aromatic); 11.35 (s, 1H, H-3). ^{13}C NMR (75 MHz, DMSO d-6) δ (ppm): 11.89 (CH_3); 20.55 (CH_3); 20.96 (CH_3); 49.31 (CH_2); 90.04 (C-oxadiazoline); 109.13 (C-5); 123.82 (C_{ph}); 124.32 (C_{ph}); 126.41 (C_{ph}); 128.12 (C_{ph});128.59 (C_{ph}); 129.02 (C_{ph}); 129.91 (C_{ph}); 131.89 (C_{ph}); 134.89 (C_{ph}); 141.17 (C-6); 148.23 (C_{ph}); 150.97 (C-2); 154.64 (C-oxadiazoline); 164.18 (C-4); 166.30 (CO acetyl); 168.55 (CO acetyl). HPLC/MS (*m*/*z*) 463.16 $(M+H)^+$, HRMS for $C_{24}H_{23}N_4O_6$: Calc 463.1612, Found 463.1611.

2-(3-Acetyl-5-phenyl-2,3-dihydro-1,3,4-oxadiazol-2-yl)-4-((5-fluoro-2,4-dioxo-3,4-dihydropyrimidin-1(2*H*)-yl) methyl) phenyl acetate (16) $R_f = 0.31$ [CH_2Cl_2/MeOH (97/3)]. Yield = 47%, $m = 66$ mg. Mp = (153–155) °C. UV (methanol) $\lambda_{max} = 278$ nm. IR υ (cm^{-1}): 3480 (NH); 1760 (C=O); 1707 (C=C); 1196 (C–N); 699 (OH phenol). ^{1}H NMR (300 MHz, DMSO d-6) δ (ppm): 2.10 (s, 3H, CH_3); 2.19 (s, 3H, CH_3); 4.86 (s, 2H, CH_2); 5.62 (s, 1H, H-aromatic); 7.18 (s, 1H, H-oxadiazoline); 7.42–7.81 (m, 8H, H-aromatic); 8.24 (d, 1H, $^3J_{H-F} = 6.9$ Hz, H-6); 11.87 (s, 1H, H-3). ^{13}C NMR (75 MHz, DMSO d-6) δ (ppm): 20.47 (CH_3); 20.96 (CH_3); 49.82 (CH_2); 90.11 (C-oxadiazoline); 123.81(C_{ph}); 124.32 (C_{ph}); 126.41 (C_{ph}); 128.11 (C_{ph}); 128.74 (C_{ph}); 129.10 (C_{ph}); 129.71 (C_{ph}); 130.01 (d, $^2J_{C-F} = 10.95$ Hz, C-6); 131.90 (C_{ph}); 134.31 (C_{ph}); 148.33 (C-2); 151.03 (C_{ph}); 154.63 (C-oxadiazoline); 141.36 (d, $^1J_{C-F} = 228.45$ Hz, C-5); 157.02 (d, $^2J_{C-F} = 28.72$ Hz, C-4); 166.31 (CO acetyl); 168.55 (CO acetyl). HPLC/MS (*m*/*z*) 467.14 $(M+H)^+$, HRMS for $C_{23}H_{20}FN_4O_6$: Calc 467.1361, Found 467.1364.

2-(3-Acetyl-5-(3-chlorophenyl)-2,3-dihydro-1,3,4-oxadiazol-2-yl)-4-((2,4-dioxo-3,4-dihydropyrimidin-1(2*H*)-yl) methyl) phenyl acetate (17) $R_f = 0.23$ [CH_2Cl_2/MeOH (97/3)]. Yield = 60%, $m = 89$ mg. Mp = (229–231) °C. UV (methanol) $\lambda_{max} = 271$ nm. IR υ (cm^{-1}): 3436 (NH); 1763 (C=O); 1689 (C=C); 689 (OH phenol). ^{1}H NMR (300 MHz, DMSO d-6) δ (ppm): 2.12 (s, 3H, CH_3); 2.19 (s, 3H, CH_3); 4.90 (s, 2H, CH_2); 5.60 (d, $^3J_{H-H} = 9$ Hz, 1H, H-5); 7.19 (s, 1H, H-oxadiazoline); 7.39–7.80 (m, 8H, H-aromatic, H-6); 11.36 (s, 1H, H-3). ^{13}C NMR (75 MHz, DMSO d-6) δ (ppm): 20.57 (CH_3); 20.94 (CH_3); 49.49 (CH_2); 90.44 (C-oxadiazoline); 101.49 (C-5); 124.35 (C_{ph}); 125.02 (C_{ph}); 125.75 (C_{ph}); 125.84 (C_{ph}); 127.99 (C_{ph});128.68 (C_{ph}); 130.05 (C_{ph}); 131.22 (C_{ph}); 131.75 (C_{ph}); 133.80 (C_{ph}); 134.77 (C_{ph}); 145.51 (C-6); 148.28 (C_{ph}); 150.98 (C-2); 153.36 (C-oxadiazoline); 163.54 (C-4); 166.49 (CO acetyl); 168.57 (CO acetyl). HPLC/MS (*m*/*z*) 483.11$(M+H)^+$, HRMS for $C_{23}H_{20}ClN_4O_6$: Calc 483.1066, Found 483.1064.

2-(3-Acetyl-5-(3-chlorophenyl)-2,3-dihydro-1,3,4-oxadiazol-2-yl)-4-((5-methyl-2,4-dioxo-3,4-dihydropyrimidin-1(2*H*)-yl) methyl) phenyl acetate (18) $R_f = 0.33$ [CH_2Cl_2/MeOH (97/3)]. Yield = 71%, $m = 106$ mg. Mp = (231–233) °C. UV (methanol) $\lambda_{max} = 277$ nm. IR υ (cm^{-1}): 3486 (NH); 1769 (C=O); 1678 (C=C); 1204 (C–N); 694 (OH phenol). ^{1}H NMR (300 MHz, DMSO d-6) δ (ppm): 1.74 (s, 3H, CH_3); 2.12 (s, 3H, CH_3); 2.19 (s, 3H, CH_3); 4.87 (s, 2H, CH_2); 7.19 (s, 1H, H-oxadiazoline); 7.66 (s, 1H, H-6); 7.39–7.76 (m, 7H, H-aromatic); 11.34 (s, 1H, H-3). ^{13}C NMR (75 MHz, DMSO d-6) δ (ppm): 11.97 (CH_3); 20.57 (CH_3); 20.94 (CH_3); 49.30 (CH_2); 90.41 (C-oxadiazoline); 109.07 (C-5); 124.33 (C_{ph}); 125.06 (C_{ph}); 125.74 (C_{ph}); 125.85 (C_{ph}); 127.99 (C_{ph}); 128.60 (C_{ph}); 130.03 (C_{ph}); 131.22 (C_{ph}); 131.75 (C_{ph}); 133.80 (C_{ph}); 134.95 (C_{ph}); 141.17 (C-6); 148.23 (C_{ph}); 150.97 (C-2); 153.42 (C-oxadiazoline aromatic); 164.18 (C-4); 166.41 (CO acetyl); 168.51 (CO acetyl). HPLC/MS (*m*/*z*) 497.12 $(M+H)^+$, HRMS for $C_{24}H_{22}ClN_4O_6$: Calc 497.1222, Found 497.1221.

2-(3-Acetyl-5-(3-chlorophenyl)-2,3-dihydro-1,3,4-oxadiazol-2-yl)-4-((5-fluoro-2,4-dioxo-3,4-dihydropyrimidin-1(2*H*)-yl) methyl) phenyl acetate (19) $R_f = 0.33$ [CH_2Cl_2/MeOH (97/3)]. Yield = 54%, $m = 81$ mg. Mp = (198–200) °C. UV (methanol) $\lambda_{max} = 279$ nm. IR υ (cm^{-1}): 3450 (NH); 1769 (C=O); 1705 (C=C); 1191 (C–N); 695 (OH phenol). ^{1}H NMR (300 MHz, DMSO d-6) δ (ppm): 2.12 (s, 3H, CH_3); 2.19 (s, 3H, CH_3); 4.86 (s, 2H, CH_2); 7.19 (s, 1H, H-oxadiazoline); 7.43–7.76 (m, 7H, H-aromatic); 8.24 (d, 1H, $^3J_{H-F} = 6$ Hz, H-6); 11.88 (s, 1H, H-3). NMR ^{13}C (75 MHz, DMSO d-6) δ (ppm): 20.48 (CH_3); 20.95 (CH_3); 49.89 (CH_2); 90.49 (C-oxadiazoline); 124.33 (C_{ph}); 125.06 (C_{ph}); 125.86 (C_{ph}); 128.00 (C_{ph}); 128.76 (C_{ph}); 129.70 (C_{ph}); 130.13 (d, $^2J_{C-F} = 1.2$ Hz, C-6); 131.23 (C_{ph}); 131.75 (C_{ph}); 133.80 (C_{ph}); 134.37 (C_{ph}); 148.33 (C-2); 149.63 (C_{ph}); 153.38 (C-oxadiazoline); 141.37(d, $^1J_{C-F} = 228.37$ Hz, C-5); 157.52 (d, $^2J_{C-F} = 21.82$ Hz, C-4); 166.47 (CO acetyl); 168.56 (CO acetyl). HPLC/MS (*m*/*z*) 501.10 $(M+H)^+$, HRMS for $C_{23}H_{19}ClFN_4O_6$: Calc 501.0972, Found 501.0970.

2-(3-Acetyl-5-(3-chlorophenyl)-2,3-dihydro-1,3,4-oxadiazol-2-yl)-4-((6-methyl-3,5-dioxo-4,5-dihydro-1,2,4-triazin-2(3*H*)-yl) methyl) phenyl acetate (20) $R_f = 0.38$ [CH_2Cl_2/MeOH (97/3)]. Yield = 60%, $m = 89$ mg. Mp = (157–158) °C. UV (methanol) $\lambda_{max} = 284$ nm. IR υ (cm^{-1}): 3449 (NH); 1769 (C=O); 1705 (C=C); 1191 (C–N); 695 (OH phenol). ^{1}H NMR (300 MHz, DMSO d-6) δ (ppm): 2.05 (s, 3H, CH_3); 2.12 (s, 3H, CH_3); 2.20 (s, 3H, CH_3); 5.02 (s, 2H, CH_2); 7.20 (s, 1H, H-oxadiazoline); 7.41–7.76 (m, 7H, H-aromatic); 12.16 (s, 1H, H-3). ^{13}C NMR (75 MHz, DMSO d-6) δ (ppm): 15.97 (CH_3); 20.45 (CH_3); 20.88 (CH_3); 51.79 (CH_2); 90.43 (C-oxadiazoline); 124.20 (C_{ph}); 125.06 (C_{ph}); 125.62 (C_{ph}); 125.94 (C_{ph}); 127.89 (C_{ph}); 128.80 (C_{ph}); 130.20 (C_{ph}); 131.23 (C_{ph}); 131.65 (C_{ph}); 133.80 (C_{ph}); 134.72 (C_{ph}); 143.66 (C-5); 148.17 (Cph); 148.88 (C-2); 153.43 (C-oxadiazoline); 157.05 (C-4); 166.47 (CO acetyl); 168.60 (CO acetyl). HPLC/MS (*m*/*z*) 498.12 $(M+H)^+$, HRMS for $C_{23}H_{21}ClN_5O_6$: Calc 498.1175, Found 498.1176.

2-(3-Acetyl-5-(4-chlorophenyl)-2,3-dihydro-1,3,4-oxadiazol-2-yl)-4-((2,4-dioxo-3,4-dihydropyrimidin-1(2*H*)-yl) methyl) phenyl acetate (21) $R_f = 0.28$ [CH_2Cl_2/MeOH (97/3)]. Yield = 59%, $m = 85$ g. Mp = (215–217) °C. UV (methanol) $\lambda_{max} = 273$ nm. IR υ (cm^{-1}): 3456 (NH); 1765 (C=O); 1667 (C=C); 1208 (C–N); 726 (OH phenol). ^{1}H NMR (300 MHz, DMSO d-6) δ (ppm): 2.11 (s, 3H, CH_3); 2.18 (s, 3H, CH_3); 4.90 (s, 2H, CH_2); 5.60 (d, $^3J_{H-H} = 7.8$ Hz, 1H, H-5); 7.18 (s, 1H, H-oxadiazoline); 7.38–7.81 (m, 7H, H-aromatic, H-6); 11.36 (s, 1H, H-3). NMR ^{13}C (75 MHz, DMSO d-6) δ (ppm): 20.57 (CH_3); 20.94 (CH_3); 49.66 (CH_2); 90.18 (C-oxadiazoline); 101.48 (C-5); 122.70 (C_{ph}); 124.34 (C_{ph}); 128.06 (C_{ph}); 128.19 (C_{ph}); 128.65 (C_{ph}); 129.32 (C_{ph}); 130.00 (C_{ph}); 134.76 (C_{ph}); 136.57 (C_{ph}); 145.51 (C-6); 148.19 (C_{ph}); 150.97 (C-2); 153.85 (C-oxadiazoline); 163.51 (C-4); 166.30 (CO acetyl); 168.54 (CO acetyl). HPLC/MS (*m*/*z*) 483.11 $(M+H)^+$, HRMS for $C_{23}H_{20}ClN_4O_6$: Calc 483.1066, Found 483.1063.

2-(3-Acetyl-5-(4-chlorophenyl)-2,3-dihydro-1,3,4-oxadiazol-2-yl)-4-((5-methyl-2,4-dioxo-3,4-dihydropyrimidin-1(2*H*)-yl) methyl) phenyl acetate (22) $R_f = 0.34$ [CH_2Cl_2/MeOH (97/3)]. Yield = 49%, $m = 73$ mg. Mp = (219–221) °C. UV (methanol) $\lambda_{max} = 278$ nm. IR υ (cm^{-1}): 3446 (NH); 1762 (C=O); 1702 (C=C); 1203 (C–N); 698 (OH phenol). ^{1}H NMR (300 MHz, DMSO d-6) δ (ppm): 1.74 (s, 3H, CH_3); 2.12 (s, 3H, CH_3); 2.18 (s, 3H, CH_3); 4.87 (s, 2H, CH_2); 7.19 (s, 1H, H-oxadiazoline); 7.38–7.81 (m, 7H, H-aromatic, H-6); 11.34 (s, 1H, H-3). ^{13}C NMR (75 MHz, DMSO d-6) δ (ppm): 11.80 (CH_3); 20.49 (CH_3); 20.94 (CH_3); 49.31 (CH_2); 90.31 (C-oxadiazoline); 109.13 (C-5); 122.70 (C_{ph}); 124.32 (C_{ph}); 127.99 (C_{ph}); 128.18 (C_{ph}); 128.59 (C_{ph}); 129.33 (C_{ph}); 129.99 (C_{ph}); 134.93 (C_{ph}); 136.58 (C_{ph}); 145.17 (C_{ph}); 148.22 (C-6); 150.97 (C-2); 153.85 (C-oxadiazoline); 164.18 (C-4); 166.36 (CO acetyl); 168.55 (CO acetyl). HPLC/MS (*m*/*z*) 497.12 $(M+H)^+$, HRMS for $C_{24}H_{22}ClN_4O_6$: Calc 497.1222, Found 497.1215.

2-(3-Acetyl-5-(4-chlorophenyl)-2,3-dihydro-1,3,4-oxadiazol-2-yl)-4-((5-fluoro-2,4-dioxo-3,4-dihydropyrimidin-1(2*H*)-yl) methyl) phenyl acetate (23) $R_f = 0.31$ [CH_2Cl_2/MeOH (97/3)]. Yield = 40%, $m = 60$ mg. Mp = (218–220) °C. UV (methanol) $\lambda_{max} = 281$ nm. IR υ (cm^{-1}): 3434 (NH); 1769 (C=O); 1709 (C=C); 1195 (C–N); 658 (OH phenol). ^{1}H NMR (300 MHz, DMSO d-6) δ (ppm): 2.11 (s, 3H, CH_3); 2.18 (s, 3H, CH_3); 4.85 (s, 2H, CH_2); 7.18 (s,

1H, H-oxadiazoline); 7.42–7.81 (m, 7H, H-aromatic); 8.23 (d, 1H, $^{3}J_{H-H}$ = 6 Hz, H-6); 11.88 (s, 1H, H-3). ^{13}C NMR (75 MHz, DMSO d-6) δ (ppm): 20.51 (CH_3); 20.94 (CH_3); 49.96 (CH_2); 90.38 (C-oxadiazoline); 122.70 (C_{ph}); 124.32 (C_{ph}); 128.06 (C_{ph}); 128.18 (C_{ph}); 128.75 (C_{ph}); 129.33 (C_{ph}); 129.71 (C_{ph}); 134.35 (C_{ph}); 136.58 (C_{ph}); 130.15 (d, $^{2}J_{C-F}$ = 4.57 Hz, C-6); 145.51 (C_{ph}); 148.32 (C-2); 153.85 (C-oxadiazoline); 141.23 (d, $^{1}J_{C-F}$ = 222.07 Hz, C-5); 157.58 (d, $^{2}J_{C-F}$ = 22.8 Hz, C-4); 166.31 (CO acetyl); 168.46 (CO acetyl). HPLC/MS (*m/z*) 501.10 $(M+H)^+$, HRMS for $C_{23}H_{19}ClFN_4O_6$: Calc 501.0972, Found 501.0970.

Materials and methods in biology

SARS-CoV-2

The used SARS-CoV-2 was derived from the Beta-Cov/Belgium/GHB-03021/2020 (EPI ISL407976|2020-02-03), which has been isolated in February 2020 from a Belgian patient having returned from Wuhan. The isolate was passed through VeroE6 cells seven times, producing two series of amino acid deletions in the spike protein [44]. Titration on Vero E6 cells was used to determine the infectious material of the viral stock.

The antiviral assay for SARS-CoV-2 is established on the previous used SARS-CoV assay [45]. After infection, the fluorescence of VeroE6-GFP cell cultures declines because of the cytopathogenic influence of the replicating virus. The cytopathogenicity is inhibited, and the fluorescent signal is maintained in the presence of an antiviral agent. To this end, VeroE6-GFP cells (kindly provided by Marnix Van Loock, Janssen Pharmaceutica, Beerse, Belgium) have been used as described previously [46, 47]. Because VeroE6 cells exhibit high chemotype efflux, the antiviral assays were carried out in the presence of the P-glycoprotein (Pgp) efflux inhibitor CP-100356 (0.5 M) [48].

VZV and HCMV

The synthetized compounds were tested against two human herpesviruses {cytomegalovirus (HCMV) strains AD-169 and Davis varicella-zoster virus strains [Oka (wild type) and 07-1 (thymidine kinase-deficient strain)]} in human embryonic lung (HEL) fibroblasts as reported previously [49].

Antileishmanial evaluation

Cell lines

The mouse monocyte/macrophage cell lines RAW 264.7 and *L. donovani* (MHOM/ET/67/HU3, also called LV9) promastigotes and axenic amastigotes were kept in accordance with the procedures presented by Pomel et al. [50]

Cytotoxicity evaluation of the compounds on RAW 264.7 macrophages

The resazurin technique, described in Pomel et al., was used to assess cytotoxicity in RAW 264.7 macrophages [50].

In vitro antileishmanial evaluation on *L. donovani* axenic amastigotes

This evaluation was performed using the SYBR Green method as previously described [50]. IC_{50} values were calculated using the IC Estimator version 1.2 software [50]. Miltefosine was used as the reference drug.

Evaluation of in vitro antileishmanial on intramacrophage amastigotes

Cytotoxicity determination, as described above, was employed to choose the highest concentrations of drug that could be investigated on the *L. donovani* intramacrophage amastigote model using RAW 264.7 cells. Macrophages were contaminated with *L. donovani* axenic amastigotes at a 10 parasites per macrophage ratio. The rate of infected macrophages was about 80% in these conditions, as well as the mean number of amastigotes for each infected macrophage was 4 to 5 in the untreated controls. The in vitro treatment was applied 24 h post-infection during 48 h. The results of the product's effect are given as rate reduction of parasite growth, measured using the SYBR Green incorporation method. The activity of the compounds is expressed as IC_{50}, calculated using the IC Estimator version 1.2 software [50]. Miltefosine was used as the reference drug.

Conclusion

In conclusion, a novel series of homonucleosides analogs of *N*-acetyl-1,3,4-oxadiazoline was synthesized and evaluated for their antileishmanial and antiviral activities against HCM, VZV, and SARS-CoV-2. Furthermore, the synthetic strategy to synthetize hybrid compounds was proved to be simple and efficient. Compound **20** was the most active with IC_{50} value less than 10 µM against the axenic and intramacrophage amastigotes forms of *L. donovani*. The absence of significant antiviral activity of this series prompts us to focus further studies on its antileishmanial potential but trying to enhance its antiviral effect. Consequently, additional chemistry work is under progress to synthesize new derivatives, to strengthen their development on a rational base, and to

optimize the antileishmanial activity and antiviral activity of the 6-azathymine as a pharmacophore.

Supplementary Information The online version contains supplementary material available at https://doi.org/10.1007/s11030-022-10548-9.

Acknowledgements The authors are extremely grateful to M. Brecht Dirix for excellent technical assistance and dedication to evaluate the anti-herpes virus activity of the derivatives. The authors would also like to thank the technical staff of the CAC (Centre of Analysis and Characterization), University Cadi Ayyad for running the spectroscopic analysis.

Funding None.

Data availability Spectroscopic data are available in the Supporting Material.Consent for publication Not applicable.

Declarations

Conflict of interest The authors declare that they have no known competing financial interests or personal relationships that could have appeared to influence the work reported in this paper.

Statement involving human and animal rights No animals/humans were used for studies that are the basis of this research.

Ethical approval Not applicable.

Informed consent Not applicable.

References

1. Hotez PJ, Nathan CL (2020) Neglected tropical diseases: public health control programs and mass drug administration. In: Hunter's tropical medicine and emerging infectious diseases. Elsevier, Inc., Amsterdam, pp 209–213
2. Kapil S, Singh PK, Silakari O (2018) An update on small molecule strategies targeting leishmaniasis. Eur J Med Chem 157:339–367
3. Croft SL, Olliaro P (2011) Leishmaniasis chemotherapy—challenges and opportunities. Clin Microbiol Infect 17:1478–1483
4. Ezra N, Ochoa MT, Craft N (2010) Human immunodeficiency virus and leishmaniasis. J Glob Infect Dis 2:248–257
5. Heirwegh E, MacLean E, He J, Kamhawi S, Sagan SM, Olivier M (2021) Sandfly Fever Sicilian Virus-*Leishmania major* co-infection modulates innate inflammatory response favoring myeloid cell infections and skin hyperinflammation. PLoS Negl Trop Dis 15:e0009638
6. Pikoulas A, Piperaki ET, Spanakos G, Kallianos A, Mparmparousi D, Rentziou G, Trakada GV (2022) Leishmaniasis and COVID-19 coinfection—a case report. IDCases 27:e01358
7. Sundar S, Sinha PK, Rai M, Verma DK, Alam KS, Chakravarty J, Vaillant M, Verma N, Pandey K, Kumari P, Lal CS, Arora R, Sharma B, Ellis S, Strub Wourgaft N, Balasegaram M, Olliaro P, Das P, Modabber F (2011) Comparison of short-course multidrug treatment with standard therapy for visceral leishmaniasis in India: an open-label, non-inferiority, randomised controlled trial. Lancet 377:477–486
8. Torres-Guerrero E, Quintanilla-Cedillo MR, Ruiz-Esmenjaud J, Arenas R (2017) Leishmaniasis: a review. F1000 Res 6:750
9. Schlecker R, Thieme PC (1988) The synthesis of antihypertensive 3-(1, 3, 4-oxadiazol-2-yl) phenoxypropanolahines. Tetrahedron 44:3289–3294
10. Bala S, Kamboj S, Kumar A (2010) Heterocyclic 1, 3, 4-oxadiazoline compounds with diverse biological activities: a comprehensive review. J Pharm Res 3:2993–2997
11. Cocohoba J, Dong BJ (2008) Raltegravir: the first HIV integrase inhibitor. Clin Ther 30:1747–1765
12. James N, Growcott JW (2009) Zibotentan endothelin ETA receptor antagonist oncolytic. Drugs Future 34:624–633
13. Fizazi K, Higano CS, Nelson JB, Gleave M, Miller K, Morris T, Nathan FE, McIntosh S, Pemberton K, Moul JW (2013) Phase III, randomized, placebo-controlled study of docetaxel in combination with zibotentan in patients with metastatic castration-resistant prostate cancer. J Clin Oncol 31:1740–1747
14. Taha M, Ismail NH, Imran S, Anouar EH, Selvaraj M, Jamil W, Ali M, Kashif SM, Rahim F, Khan KM, Adenan MI (2017) Synthesis and molecular modeling studies of phenyl linked oxadiazoline–phenylhydrazone hybrids as potent antileishmanial agents. Eur J Med Chem 126:1021–1033
15. Taha M, Ismail NH, Ali M, Rashid U, Imran S, Uddin N, Khan KM (2017) Molecular hybridization conceded exceptionally potent quinolinyl–oxadiazoline hybrids through phenyl linked thiosemicarbazide antileishmanial scaffolds: in silico validation and SAR studies. Bioorg Chem 71:192–200
16. Ali OM, Amer HH, Abdel Rahman AH (2007) Synthesis and antiviral evaluation of sugar uracil-1-ylmethylhydrazones and their oxadiazoline derivatives. Synthesis 2007:2823–2828
17. Mallikarjuna BP, Sastry BS, Suresh Kumar GV, Rajendraprasad Y, Chandrashekar SM, Sathisha K (2009) Synthesis of new 4-isopropylthiazole hydrazide analogs and some derived clubbed triazole, oxadiazoline ring systems—a novel class of potential antibacterial, antifungal and antitubercular agents. Eur J Med Chem 44:4739–4746
18. Joshi SD, Vagdevi HM, Vaidya VP, Gadaginamath GS (2008) Synthesis of new 4-pyrrol-1-yl benzoic acid hydrazide analogs and some derived oxadiazoline, triazole and pyrrole ring systems: a novel class of potential antibacterial and antitubercular agents. Eur J Med Chem 4:1989–1996
19. Rollas S, Nehir G, Erdeniz H (2002) Synthesis and antimicrobial activity of some new hydrazones of 4-fluorobenzoic acid hydrazide and 3-acetyl-2, 5-disubstituted-1, 3, 4-oxadiazolines. Il Farmaco 57:171–174
20. Popiolek L, Biernasiuk A, Paruch K, Malm A, Wujec M (2019) Synthesis and in vitro antimicrobial activity screening of new 3-acetyl-2, 5-disubstituted-1, 3, 4-oxadiazoline derivatives. Chem Biodivers 16:e1900082
21. Kaymakçioglu BK, Emre EEO, Unsalan SU, Tabanca N, Iqrar Khan S, Wedge ED, Iscan G, Demirci F, Rollas S (2012) Synthesis and biological activity of hydrazide–hydrazones and their corresponding 3-acetyl-2, 5-disubstituted-2, 3-dihydro-1, 3, 4-oxadiazolines. Med Chem Res 21:3499–3508
22. Grover J, Bhatt N, Kumar V, Patel NK, Gondaliya BJ, Elizabeth Sobhia M, Bhutani KK, Jachak SM (2015) 2,5-Diaryl-1,3,4-oxadiazoles as selective COX-2 inhibitors and anti-inflammatory agents. RSC Adv 5:45535–45544
23. Sharma V, Chitranshi N, Agarwal AK (2014) Significance and biological importance of pyrimidine in the microbial world. Int J Med Chem 2014:1–31
24. Nakagawa Y, Bobrov S, Semer CR, Kucharek TA, Harmoto M (2004) Fungicidal pyrimidine derivatives. United States Patent

25. Cieplik J, Stolarczyk M, Pluta J, Gubrynowicz O, Bryndal I, Lis T, Mikulewicz M (2015) Synthesis and antibacterial properties of pyrimidine derivatives. Acta Pol Pharm 72:53–64
26. Thomson JM, Lamont IL (2019) Nucleoside analogues as antibacterial agents. Front Microbiol 10:952
27. Vega S, Alonso J, Diaz JA, Junquera F (1990) Synthesis of 3-substituted-4-phenyl-2-thioxo-1, 2, 3, 4, 5, 6, 7, 8-octahydrobenzo [4, 5] thieno [2, 3-á] pyrimidines. J Heterocycl Chem 27:269–273
28. Luo MZ, Liu MC, Mozdziesz DE, Lin TS, Dutschman GE, Gullen EA, Cheng YC, Sartorelli AC (2000) Synthesis and biological evaluation of L- and D-configuration 1, 3-dioxolane 5-azacytosine and 6-azathymine nucleosides. Bioorg Med Chem Lett 10:2145–2148
29. El Mansouri A, Oubella A, Dânoun K, Ahmad M, Neyts J, Jochmans D, Snoeck R, Andrei G, Morjani H, Zahouily M, Lazrek HB (2021) Discovery of novel furo[2,3-d] pyrimidin-2-one–1,3,4-oxadiazole hybrid derivatives as dual antiviral and anticancer agents that induce apoptosis. Arch Pharm 354:2100146
30. Ae EM, Oubella A, Maatallah M, AitItto MY, Zahouily M, Morjani H, Lazrek HB (2020) Design, synthesis, biological evaluation and molecular docking of new uracil analogs-1, 2, 4-oxadiazoline hybrids as potential anticancer agents. Bioorg Med Chem Lett 30:127438
31. El Mansouri A, Maatallah M, Ait Benhassou H, Moumen A, Mehdi A, Snoeck R, Andrei G, Zahouily M, Lazrek HB (2020) Design, synthesis, chemical characterization, biological evaluation, and docking study of new 1,3,4-oxadiazole homonucleoside analogs. Nucleosides Nucleotides Nucleic Acids 39:1088–1107
32. Vincent IM, Barrett MP (2015) Metabolomic-based strategies for anti-parasite drug discovery. J Biomol Screen 20:44–55
33. Sharma M, Chauhan K, Shivahare R, Vishwakarma P, Suthar MK, Sharma A, Gupta S, Saxena JK, Lal J, Chandra P, Kumar B, Chauhan PMS (2013) Discovery of a new class of natural product-inspired quinazolinone hybrid as potent antileishmanial agents. J Med Chem 56:4374–4392
34. Suryawanshi SN, Kumar S, Shivahare R, Pandey S, Tiwari A, Gupta S (2013) Design, synthesis and biological evaluation of aryl pyrimidine derivatives as potential leishmanicidal agents. Bioorg Med Chem Lett 23:5235–5238
35. Chauhan K, Sharma M, Shivahare R, Debnath U, Gupta S, Prabhakar YS, Chauhan PM (2013) Discovery of triazine mimetics as potent antileishmanial agents. ACS Med Chem Lett 4:1108–1113
36. El Mansouri A, Zahouily M, Lazrek HB (2019) HMDS/KI a simple, a cheap and efficient catalyst for the one-pot synthesis of *N*-functionalized pyrimidines. Synth Commun 49:1802–1812
37. Guieu S, Rocha J, Silva AMS (2013) Synthesis of unsymmetrical methylenebisphenol derivatives. Synlett 24:762–764
38. Marhadour S, Marchand P, Pagniez F, Bazin MA, Lozach CPO, Ruchaud S, Antoine M, Meijer L, Rachidi N, Le Pape P (2012) Synthesis and biological evaluation of 2,3-diarylimidazo[1,2-a] pyridines as antileishmanial agents. Eur J Med Chem 58:543–556
39. Gamal El Din MM, El Gamal MI, Abdel Maksoud MS, Ho Yoo K, Oh CH (2015) Synthesis and broad-spectrum antiproliferative activity of diarylamides and diarylureas possessing 1,3,4-oxadiazoline derivatives. Bioorg Med Chem Lett 25:1692–1699
40. Zhao J, Liu Q, Yi D, Li Q, Guo S, Ma L, Zhang Y, Dong D, Guo F, Liu Z, Wei T, Li X, Cen S (2022) 5-Iodotubercidin inhibits SARS-CoV-2 RNA synthesis. Antiviral Res 198:105254
41. Dustin LB, Bartolini B, Capobianchi MR, Pistello M (2016) Hepatitis C virus: life cycle in cells, infection and host response, and analysis of molecular markers influencing the outcome of infection and response to therapy. Clin Microbiol Infect 22:826–832
42. Elfiky AA (2020) Ribavirin, Remdesivir, Sofosbuvir, Galidesivir, and Tenofovir against SARS-CoV-2 RNA dependent RNA polymerase (RdRp): a molecular docking study. Life Sci 253:117592
43. Parsons TL, Kryszak LA, Marzinke MA (2021) Development and validation of assays for the quantification of β-D-N4-hydroxycytidine in human plasma and β-D-N4-hydroxycytidine-triphosphate in peripheral blood mononuclear cell lysates. J Chromatogr B 1182:122921
44. Boudewijns R, Thibaut HJ, Kaptein SJF, Li R, Vergote V, Seldeslachts L, Weyenbergh JV, De Keyzer C, Bervoets L, Sharma S, Liesenborghs L, Ma J, Jansen S, Van Looveren D, Vercruysse T, Wang X, Jochmans D, Martens E, Roose K, De Vlieger D, Schepens B, Van Buyten T, Jacobs S, Liu Y, Martí Carreras J, Vanmechelen B, Wawina Bokalanga T, Delang L, Rocha Pereira J, Coelmont L, Chiu W, Leyssen P, Heylen E, Schols D, Wang L, Close L, Matthijnssens J, Van Ranst M, Compernolle V, Schramm G, Van Laere K, Saelens X, Callewaert N, Opdenakker G, Maes P, Weynand B, Cawthorne C, Vande Velde G, Wang Z, Neyts J, Dallmeier K (2020) STAT2 signaling restricts viral dissemination but drives severe pneumonia in SARS-CoV-2 infected hamsters. Nat Commun 11:5838
45. Ivens T, Van den Eynde C, Van Acker K, Nijs E, Dams G, Bettens E, Ohagen A, Pauwels R, Hertogs K (2005) Development of a homogeneous screening assay for automated detection of antiviral agents active against severe acute respiratory syndrome-associated coronavirus. J Virol Methods 129:56–63
46. Do TND, Donckers K, Vangeel L, Chatterjee AK, Gallay PA, Bobardt MD, Bilello JP, Cihlar T, De Jonghe S, Neyts J, Jochmans D (2021) A robust SARS-CoV-2 replication model in primary human epithelial cells at the air liquid interface to assess antiviral agents. Antiviral Res 192:105122
47. Abdelnabi R, Foo CS, Jochmans D, Vangeel L, De Jonghe S, Augustijns P, Mols R, Weynand B, Wattanakul T, Hoglund RM (2022) The oral protease inhibitor (PF-07321332) protects Syrian hamsters against infection with SARS-CoV-2 variants of concern. Nat Commun 13:1–9
48. Hoffman RL, Kania RS, Brothers MA, Davies JF, Ferre RA, Gajiwala KS, He M, Hogan RJ, Kozminski K, Li LY, Lockner JW, Lou J, Marra MT, Mitchell LJ Jr, Murray BW, Nieman JA, Noell S, Planken SP, Rowe T, Ryan K, Smith GJ III, Solowiej JE, Steppan CM, Taggart B (2020) Discovery of ketone-based covalent inhibitors of coronavirus 3CL proteases for the potential therapeutic treatment of COVID-19. J Med Chem 63:12725–12747
49. Yuan W, Chen X, Liu N, Wen Y, Yang B, Andrei G, Snoeck R, Xiang Y, Wu YW, Jiang Z, Schols D, Zhang Z, Wu Q (2019) Synthesis, anti-varicella-zoster virus and anti-cytomegalovirus activity of 4,5-disubstituted 1,2,3-(1*H*)-triazoles. Med Chem 15:801–812
50. Pomel S, Cojean S, Pons V, Cintrat JC, Nguyen L, Vacus J, Pruvost A, Barbier J, Gillet D, Loiseau PM (2021) An adamantine derivative as a drug candidate for the treatment of visceral leishmaniasis. J Antimicrob Chemother 76:2640–2650